



Controlling and monitoring of a solar-powered DC motor using a wireless sensor network

Salim & Jyoti Ohri

To cite this article: Salim & Jyoti Ohri (2022): Controlling and monitoring of a solar-powered DC motor using a wireless sensor network, IETE Journal of Research, DOI: [10.1080/03772063.2022.2073274](https://doi.org/10.1080/03772063.2022.2073274)

To link to this article: <https://doi.org/10.1080/03772063.2022.2073274>



Published online: 24 May 2022.



Submit your article to this journal [↗](#)



Article views: 10



View related articles [↗](#)



View Crossmark data [↗](#)

Controlling and monitoring of a solar-powered DC motor using a wireless sensor network

Salim¹ and Jyoti Ohri²

¹Electrical and Electronics Engineering, KIET Group of Institutions, Delhi-NCR Ghaziabad, India; ²Electrical Engineering Department, National Institute of Technology, Kurukshetra, India

ABSTRACT

Due to the economic challenges of soaring oil costs and natural concerns, India faces an enormous growth in renewable energy resources. The solar photovoltaic technology, as a clean and green energy source, plays a critical role in addressing any country's power shortage. Before mounting a PV system at any location, modeling, simulation, and analysis of solar photovoltaic (PV) generators is a critical phase that helps to understand the behavior and characteristics of the system in real-world climatic conditions. A solar panel, buck-boost converter, separately excited (S.E) DC motor, and controllers, such as Proportional Integral Derivative (PID), Fuzzy, fuzzy based on PID (FPID), and Artificial Neural Network (ANN) controllers are all included in the proposed system. Because compared to other controllers, the ANN controller produces better results. It was designed to deal with system non-linearity and system-related ambiguity. Wireless sensor network (WSN) and Data Dashboard for LabVIEW are used to monitor and control the system.

KEYWORDS

WSN; solar energy; MPPT; Data Dashboard; FPID; ANN

1. INTRODUCTION

With growing concerns about air pollution and global warming, clean renewable energy sources are expected to play an important role or play a major role in the global strength of the future. If we want to ensure that every citizen in the country has access to electricity 24 h a day, seven days a week, the most promising solution is solar power. Geographically, India has ideal properties for solar energy. Solar radiation provides the core of the most promising and lasting light source, and its superior performance can be leveraged by artificial intelligence to achieve the best possible performance. As the acceptance of LEDs, low voltage electronics and efficient DC motor technology increases, household energy needs to be covered using direct current flowing directly from solar panels. This can reduce energy consumption by more than 50%. A photovoltaic system converts solar radiation into direct current. The use of PV structures as a power source for electrical machinery is seen as a promising region for PV packaging as the PV market continues to boom. Dynamic and steady-state characteristics of photovoltaic S.E. DC motors for various solar intensities, special load conditions, and special device control have been proposed. Today, the mechanical technology has reached high peak utilization, efficiency and cost analysis have skyrocketed, and is a major concern in the development of low-power motor drives for industrial and home

use. The MPPT technology is used to obtain the maximum power output of a PV system by adjusting the load resistance to obtain the maximum power. [1,2]. A cotton core-based heat distributor reduces temperature by 12% [3]. This article will use solar energy to power a DC motor. This motor runs on a fuzzy PID logic (FPID) controller instead of a traditional controller to improve speed accuracy [2]. Various cooling methods are used to improve the efficiency of solar collectors [4-6]. This article compares the various efficiencies of G²GPVT and G²T, and finds that the efficiency of G²GPVT is superior to that of G²T [7-9]. Cost reductions for solar panel glass and back sheets are discussed [10,11]. Glaze and non-glaze thermoelectric PV panels can also be examined. [12,13] describes the data acquisition system that LabVIEW uses for solar cell models [14]. Portable data acquisition systems are designed for photovoltaic power plants. Annual data from the plant are compared to commercial devices [15]. Matlab-based and MATLAB-based solar cell models are described [16]. A 150W solar panel with the PWM technology is simulated in LabVIEW [17,18]. Various issues are discussed when networking solar power and grids [19]. PV energy is an important part of our energy consumption and our renewable energy network. With the rapid development of technology, the price of PV modules has fallen, and PV modules have become more efficient. More amount of money is

invested in off-grid PV systems and grid-connected PV networks [20,21]. There is a temporary problem with the P & O algorithm that uses the controller during the abrupt changes in radiation that contribute to the distortion of the operating parameters of the PV system [22]. In addition, power is lost because the terminal voltage fluctuates throughout the MPP. The minimum disturbance phase size can be used to compensate for these vibrations. The INC algorithm using the Proportional Integral (PI) controller is excellent. Rapid changes in irradiance reduce crack vibrations through the MPP. Therefore, the INC algorithm often separates from the MPP during a sudden change in irradiance, thus balancing response and swing velocity. According to [23], these algorithms cannot quickly and reliably track full power due to vibrations at the highest point. The human brain's network of biological neurons breathes life into the ANN system. It is used for the formation and evaluation of the non-linear relationship between I-V and P-V in a photovoltaic system. ANN constantly learns how to adapt the operation of a PV system to maximum performance by capturing inputs such as input current, input voltage, irradiance, temperature, and measurement data [24]. FLC designs can be modeled using ANN, which increases accuracy and simplifies the implementation of the converter [25]. In actual operation conditions, the ANN-based MPPT can monitor the MPP with minimal stabilization time and low ripple [26]. The proposed model is shown in Figure 1. The dissertation is divided into the following parts:

- Calculations of a Photovoltaic Cell
- S.E DC Motor Algebraic Approach
- MPPT Control Algorithm
- FPID (Fuzzy-based PID) Controller
- ANN (Artificial Neural Network) Controller
- WSN (Wireless Network System)
- Simulation Results

Monitoring of solar characteristics has been remotely observed using the Data dashboard, and the speed of the motor can also be controlled remotely.

2. CALCULATION OF THE PHOTOVOLTAIC CELL

Solar cells are the basic device for converting photon energy into green power when connected in series and parallel as PV modules. To build a PV system, these modules are combined in series and parallel to produce clean, green power. Only one solar cell can be represented as a constituent electrical circuit. The practical model includes a diode, a photocurrent, a serial resistor and a

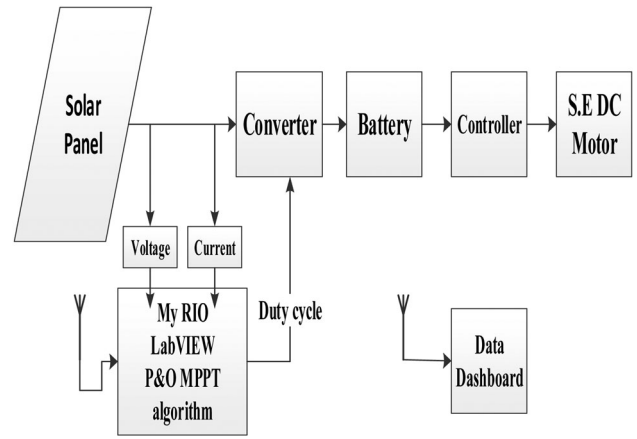


Figure 1: W-N-Based Solar-powered S.E DC motor model

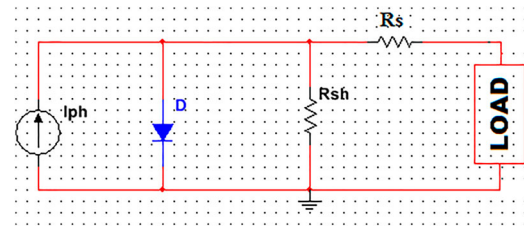


Figure 2: Single-diode identical model for photovoltaic cell

shunt resistor. This combination is referred to as a single diode solar cell model [27]. The simplified circuit model of the solar panel is shown Figure 2. A photovoltaic device can be considered an ideal solar cell with a current source (I_{ph}) parallel to the diode and series and shunt resistance [28,29], as shown in Figure 2. Due to the simplicity and accuracy of the mathematical calculations, one diode model has been described to simulate a solar panel [30,31].

The output current of the solar PV Panel

$$I = N_p \times \left[I_{ph} + I_0 - I_0 \times \exp\left(\frac{V \times N_p + N_s \times I \times R_s}{n \times V_t \times N_p \times N_s}\right) \right] - I_{sh} \quad (1)$$

where

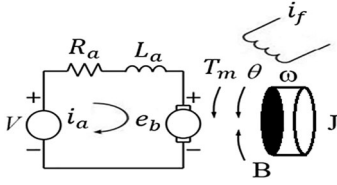
$$V_t = \frac{k \times T}{q} \quad (2)$$

$$I_{sh} = \frac{V \times N_p + N_s \times I \times R_s}{R_{sh} \times N_s} \quad (3)$$

Here, parallelly connected PV cells are denoted as N_p , series resistance as $R_s(\Omega)$, shunt resistance as $R_{sh}(\Omega)$ and diode thermal voltage as $V_t(V)$.

Table 1: Electrical parameter of a 200 W solar panel module

Parameter	Symbol	Value
Open circuit voltage	V_{oc}	32.9V
Optimum operation voltage	V_m	26.4V
Short circuit current	I_{sc}	8.21A
Open operation current	I_m	7.58A
Band gap energy	E_{g0}	1.1eV
Boltzmann Constant	K	$1.38 \times 10^{-23} \text{J/K}$
Coulomb Constant	q	$1.6 \times 10^{-19} \text{C}$
Reference temperature	T_r	298 *K
Ideal factor	n	1.3
Module cell in series	N_s	54
Module cell in Parallel	N_p	1
Temperature coefficient	K_i	0.0032
Series resistance	R_s	0.221 Ω
Shunt resistance	R_{sh}	415.405 Ω
Rated power	P_m	200W

**Figure 3:** Identical circuit for Separately Excited DC motor [32].

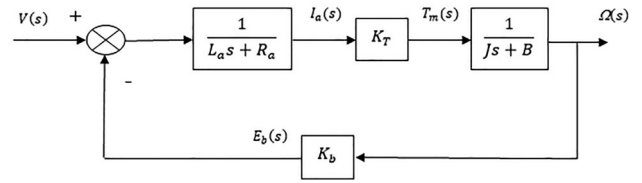
PV Cell voltage output

$$V = N_s \times \left[n \times V_t \times \log \left\{ \frac{I + I_{sh} - N_p \times I_{ph}}{N_p \times I_0} + 1 \right\} - \frac{I \times R_s}{N_p} \right] \quad (4)$$

To develop a model and perform simulations, a 200W solar panel is selected. This module is made up of 54 polysilicon solar cells connected in series. This module has high conversion efficiency, and its main characteristics are shown in Table 1. The below parameters are under STC conditions.

3. S.E DC MOTOR ALGEBRAIC APPROACH

The operation of a DC motor depends on the power supply and the magnetic flux generated by the power supply. First, the motor is excited by a power source separate from the field, creating magnetic flux in the field. By supplying to the armature, current flows through the armature, and magnetic flux flows through the rotor. The interaction between these two magnetic fluxes produces the torque that initiates the rotation of the rotor. The excitation current is independent of the armature current. Therefore, this motor can be controlled by armature control without disturbing the field magnetic flux [1] (Figure 3).

**Figure 4:** DC motor armature control block diagram representation

Back EMF e_b has a direct relation to angular speed ω

$$e_b(t) = K_b \frac{d(t)}{dt} = K_b(t) \quad (5)$$

Using KVL

$$V(t) = R_a i_a(t) + L_a \frac{di_a(t)}{dt} + e_b(t) \quad (6)$$

$V(t)$ is the output voltage of the solar panel.

Torque was obtained using Newton's law

$$T_m(t) = J \frac{d^2(t)}{dt^2} + B \frac{d}{dt} = K_T i_a(t) \quad (7)$$

The Block Diagram representation of the DC motor is shown in [33] Figure 4.

Angular speed and Input voltage relation in terms of transfer function [8]

$$G(s) = \frac{\omega(s)}{V(s)} = \frac{K_T}{(L_a s + R_a)(J s + B) + K_b K_T} \quad (8)$$

$$= \frac{0.028}{(4.47296 \times 10^{-6})s^2 + 3.1820410 \times 10^{-5}s + 0.00078994}$$

4. MPPT CONTROL ALGORITHM (PERTURB AND OBSERVE)

The P&O method is the most widely used MPPT algorithm. This algorithm employs a straightforward feedback scheme and a few measurable parameters. In this method, the array voltage is perturbed regularly, and the output power is compared to that of the previous perturbation period. For MPPT, various algorithm methods can be used. The most well-known techniques are perturbed and observed (P&O). To ensure maximum power, this algorithm alters the operating voltage. The P&O algorithm is also known as "hill-climbing," but depending on how it is implemented, both terms refer to the same algorithm [34,35]. The proposed algorithm

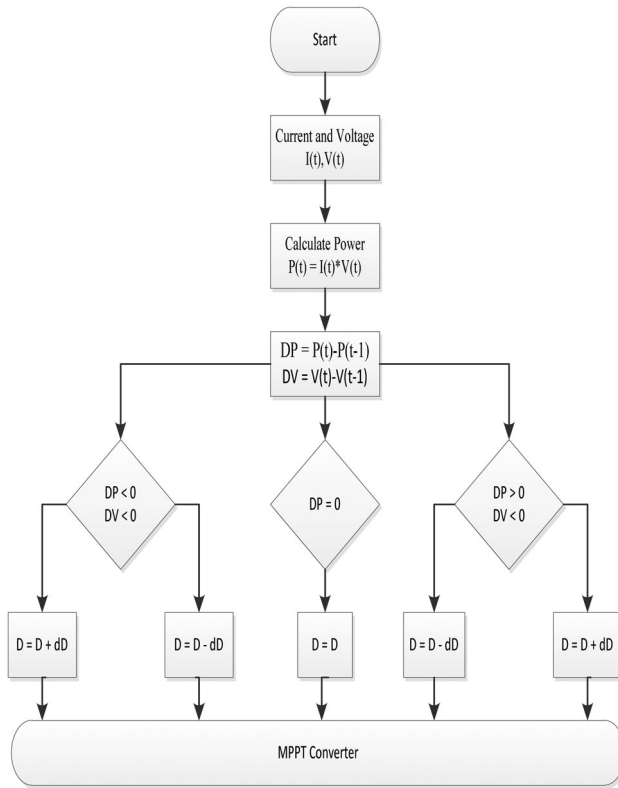


Figure 5: P&O algorithm flow diagram

differs from other techniques in that it is used to control the power drawn from the PV directly. The proposed MPPT has a lot of benefits, including simplicity, fast convergence, and independence from PV array characteristics [7]. The algorithm is easy to understand using the following flowchart in Figure 5.

The module voltage was perturbed periodically, and its cell output power was correlated with the previous cycle. Perturbation and observation continuously increase or decrease the panel voltage and compare the current output power of the PV module with the previous [1]. MPP tracking using the P&O algorithm is performed in a closed-loop [36]. The panel operating power is calculated using a voltage and a current sensor (ACS712). The operation of the Perturb & Observe (P&O) algorithm is shown in Figure 5.

5. FPID CONTROLLER

Fuzzy plus PID (FPID) controller provides better results than conventional controller for complex and nonlinear systems. FPID controller provides simple and effective control; it can improve dynamic and transient response characteristics. FPID is a combination of Fuzzy and PID controllers. Here proportional, integral, and derivative gains of the PID controller are set by a fuzzy system [37].

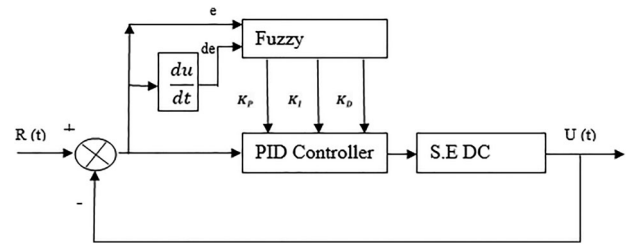


Figure 6: Fuzzy tuned PID controller

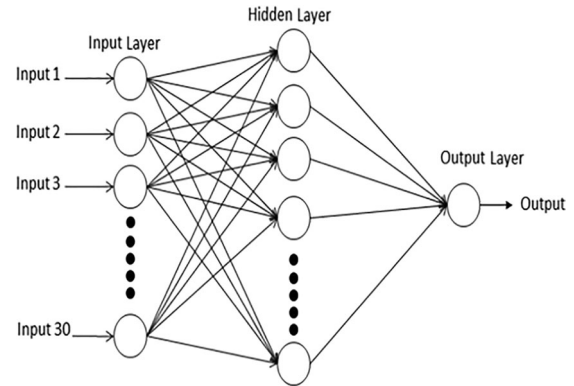


Figure 7: Simple ANN structure

The structure of Fuzzy-based PID controller is presented in Figure 6.

6. ARTIFICIAL NEURAL NETWORK (ANN)

ANN is famous for its potential to deal with the demands of changing environment. Like the human brain, ANN has trouble solving strategies. ANN has neurons, which can travel through linkages just like the brain. Neurons can communicate with each other and pass information. In supervised learning ANN, there is a “supervisor”, which provides information to the network to derive it from following the true function. Here input vectors are applied to the network, then the output of the ANN is compared with the true value (provided by the supervisor). Based on the difference between input and output, the supervisor defines an error criterion. Based on the error criterion, the weights of the ANN are updated. The process is repeated continuously until the error is minimized or a supervised network is achieved. Supervised learning ANN network learns from the environment and improves its performance from time to time. The supervised learning ANN network works with a backpropagation neural network model that contains only three layers. H. Inputs, outputs, and intermediate layers (hidden layers), as shown in Figure 7.

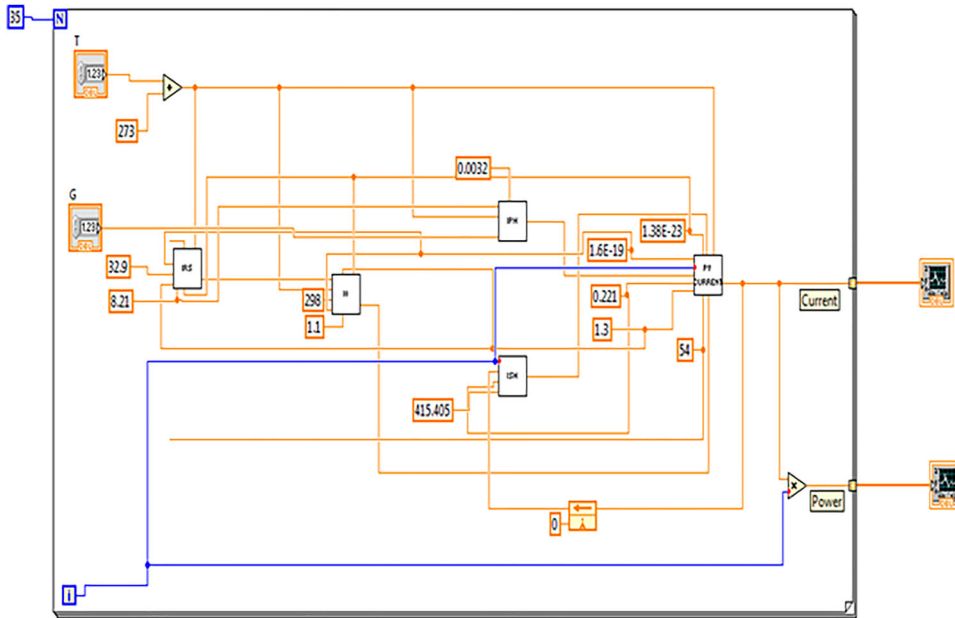


Figure 8: LabVIEW block diagram intended for a solar photovoltaic module

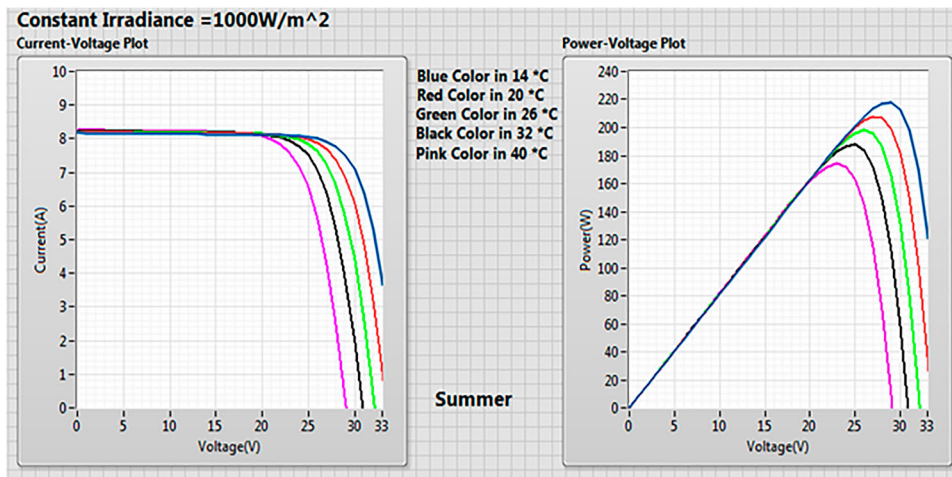


Figure 9: I-V and P-V curve for summer (North India)

7. WIRELESS NETWORK SYSTEM (WSN)

National Instruments wireless network system includes two main parts:

- (a) Gateway (WSN-9792)
- (b) Node (WSN-3202)

7.1 WSN-9792 (Gateway)

WSN-9792 is a programmable real-time controller. The processor has a 533 MHz speed. The gateway can communicate up to 36 WSN nodes.

7.2 WSN-3202 (Node)

WSN-3202 is a 16-bit analog input node. It has four analog input channels (± 10 V) and four bidirectional digital channels (30 V max). Node has a range of up to 300 m.

7.3 Data Dash Board

LabVIEW is the most touch-ready language on the planet [7]. For wireless monitoring and controlling, Data Dashboard for LabVIEW is used [38]. In Data Dashboard, custom and portable views are created. Using shared

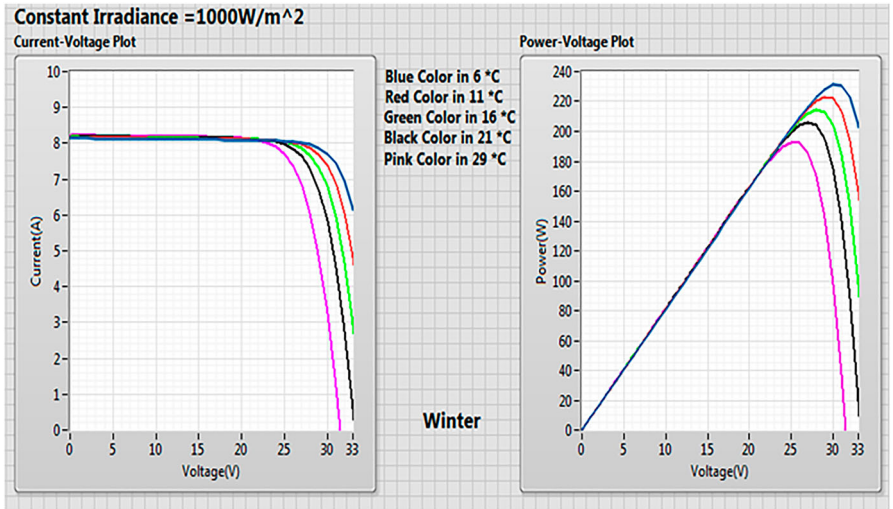


Figure 10: I-V and P-V curve for winter (North India)

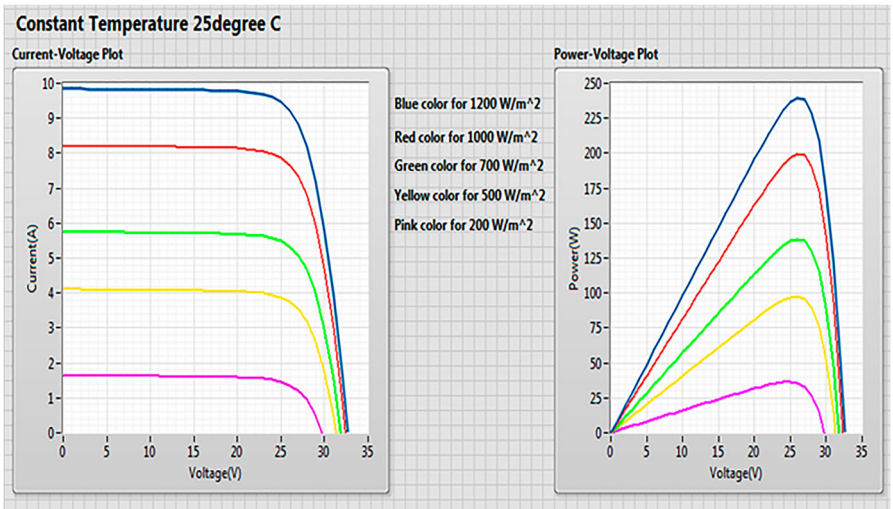


Figure 11: P-V and I-V curves under different irradiance levels

Irradiance	Power (W)								
	1000W/m2	900W/m2	800W/m2	700W/m2	600W/m2	500W/m2	400W/m2	300W/m2	200W/m2
10°C	224.429	201.76	178.996	156.146	133.219	110.221	87.1587	64.0389	41.401
15°C	216.155	194.307	172.362	150.328	128.214	106.026	83.7714	61.5458	39.761
20°C	207.843	186.818	165.693	144.477	123.178	101.803	80.3589	59.0911	38.1023
25°C	199.5	179.299	158.995	138.598	118.116	97.5559	76.9244	56.6162	36.4265
30°C	191.13	171.753	152.272	132.696	113.032	93.2886	73.4758	54.1232	34.7355
35°C	182.741	164.189	145.531	126.776	107.931	89.0054	70.1608	51.6143	33.0634
40°C	174.34	156.611	138.776	120.842	102.818	84.7112	66.8304	49.0923	31.4333

Figure 12: Output power of the solar panel

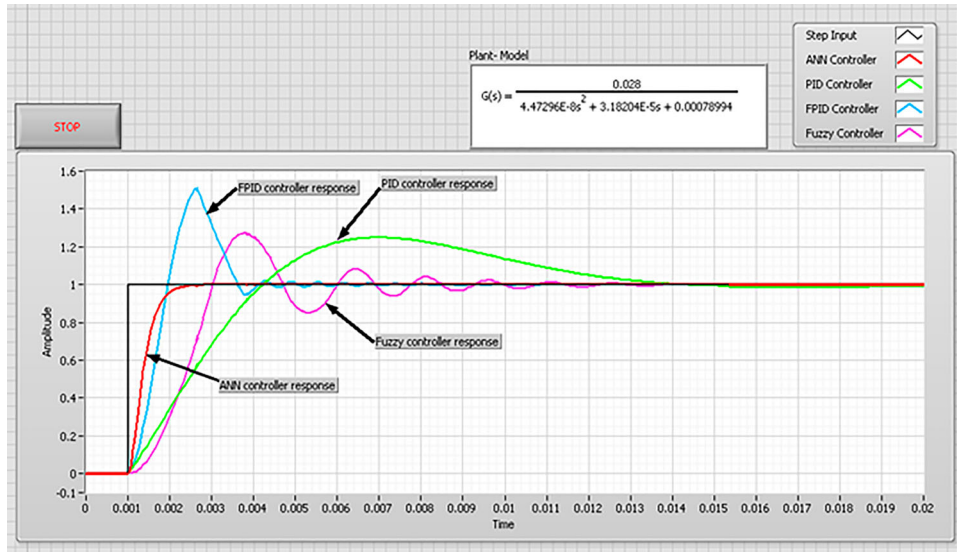


Figure 13: S.E DC motor control using Fuzzy and FPID controller

variables, data are published to the cloud directly, and data can be visualized on any Tablet or Mobile equipped with Data Dashboard [39]. Data Dashboard has control and indicators, including LEDs, charts, graphs, slider, switches, etc. It can provide a central location for various data for monitoring and analyzing system performance [40,41] Real-time monitoring reduces analysis time and long communication lines.

8. SIMULATION OUTCOMES

Table 1 shows the specifications and constant values for solar PV modules. As illustrated in Figure 7, the final PV solar module model was created in the LabVIEW environment [37], with input parameters irradiation and temperature and output results as current (I) and power (P). Figure 7 depicts a block diagram of LabVIEW programming of a PV module using various saturation current, photocurrent, and reverse saturation current formulas (Figure 8).

The PV module model is developed in a LabVIEW environment using the solar cell formula. In LabVIEW, a simulation model of a solar PV module is created using the GUI to study the effect of various parameters, such as temperature and irradiance.

8.1 Effect of Temperature variations

Standard test conditions for solar panel (STC)

Temperature = 25°C

Irradiance = 1000 W/m²

The irradiance level is set to a constant value 1000 W/m² to investigate the effect of temperature variation. Temperatures in the Ghaziabad region of INDIA range from 10°C to 44°C. So different temperatures (such as 11°C, 21°C, 26°C, 32°C, and 40°C) were used to determine the effect of temperature on solar panels depending on the winter and summer seasons (Figures 9 and 10).

The results show that for a fixed irradiance level of 1000 Wm², there is a large variation in power in the summer season (14°C to 40°C) compared to the winter season (6°C to 28°C) because temperature variations in the summer are greater. With increasing temperature, the voltage decreases rapidly, while the current varies only slightly, resulting in a decrease in solar cell power [6].

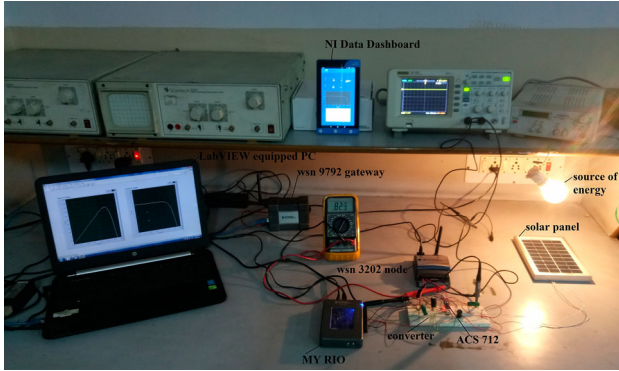
8.2 Effect of Irradiance variations

The average solar radiation that enters the Earth's atmosphere is 1361 W/m². On a clear day, the intensity of the sun's rays is reduced by the ecosystem, and the intensity of radiations at the surface is around 1000 W/m². To investigate the effect of varying irradiance, the temperature level is set to a constant value = 25°C (Figure 11).

Figure 12 depicts the output power of a solar panel as it varies with solar irradiance and temperature. The temperature range for temperature variation is from 10°C to 40°C. The irradiance variation range is 1000 W/m² to 200 W/m². As illustrated in Figure 12, the effect of irradiance variation is greater than the effect of temperature change.

Table 2: Transient response specifications for different controllers

Transient Response Specifications	PID	Fuzzy	FPID	ANN
Damping ratio	0.68	0.77	0.8	0.82
Peak time (s)	0.007	0.0038	0.0026	0.0024
Rise time (s)	0.0043	0.003	0.0019	0.0016
Settling time (s)	0.0144	0.0114	0.0084	0.003
Dead time (s)	0.0035	0.0031	0.0023	-

**Figure 14:** Hardware implementation of solar monitoring and MPPT controller using WSN and Data Dashboard

8.3 S.E DC motor control using a controller

S.E DC motor using math script has been modeled in the Block diagram window of LabVIEW [42,43]. Speed control of S.E DC motor has been performed in control and simulation loop using Fuzzy and Fuzzy PID controller blocks [20].

Step response specifications of S.E DC motor using Fuzzy and Fuzzy PID controller for speed control comparison are shown in Table 2, and response specifications of S.E DC motor using Fuzzy and Fuzzy PID controller for speed control are shown in Figure 13.

Table 2 shows that transient response specifications obtained using Artificial Neural Network-Based controlled are better than other controllers. There is no overshoot present in the case of the ANN controller. Major improvement occurred in settling time, 64.82% improvement using ANN compared to FPID. 2.5% improvement in Damping Ratio, 7.6% improvement in Peak time, 15.78% improvement in Rise time performed by ANN controller compared to FPID controller in speed control of the DC motor (Figure 14).

8.3.1 Hardware Implementation

For hardware implementation, a 5W solar panel is used. The 100W bulb is used to provide radiation for the solar panel. The current and voltage are taken from the solar panel. To measure current, an ACS 712 sensor is used,

and a voltage divider circuit is used to measure voltage (with a scale factor of 10). The outputs of these sensors are transmitted to the analog node WSN 3202. Using the WSN 9792 Gateway Node, data were collected in a LabVIEW-equipped laptop computer. NI My RIO provides a variable duty cycle to the converter based on the P&O MPPT algorithm. Here, depending on the input signal (current and voltage), the P&O algorithm changes the duty cycle of the buck-boost converter. Variable duty cycle is powered by NI myRIO. For myRIO, there are two input signals (analog) and one output signal (PWM). The solar panel voltage and current source are monitored using the NI Data Panel app and the WSN button.

As illustrated in Figure 15 The speed of the DC motor is rad/s, the current is A, the torque of the DC motor is Nm, and the voltage of the solar PV panel is V. With varying irradiance levels, the output voltage of a solar PV panel remains almost constant at 20 V. Still, the current of a solar PV panel varies from 4 to 6A, the speed of a DC motor remains relatively steady at 73 rad/s, and the torque ranges from 1 to 2.5 Nm.

As illustrated in Figure 16 with varying irradiance levels, the output voltage of a solar PV panel remains almost constant at 30 V, but the current of a solar PV panel varies from 2 to 9A, the speed of a DC motor remains relatively steady at 112 rad/s, and the torque ranges from 1 to 3 Nm.

8.3.2 NI Data Dashboard

The output parameter of the solar panel is monitored using NI Data Dashboard. The national instruments data dashboard is used to monitor temperature, humidity, current, and voltage of the solar panel.

8.3.3 Images for Data Dashboard for LabVIEW

The Lenovo tablet has a data dashboard application installed (Android-based). Figure 17 shows the addition of controls and indicators to the page. Connect these controls and indicators to shared variables and run the data dashboard. Now evaluate and control the given system.

9. CONCLUSION

In this article, it has been illustrated that for variable intensity and variable weather conditions fixed power is delivered to the S.E DC motor. Simulation work is done to monitor and control a 200W solar panel. The hardware for a 5W solar panel has been managed to complete. The control of the S.E DC motor is done separately using different controllers. Compatibility for the proposed system, regardless of the climate circumstance, has been verified using LabVIEW-based simulation results. The proposed

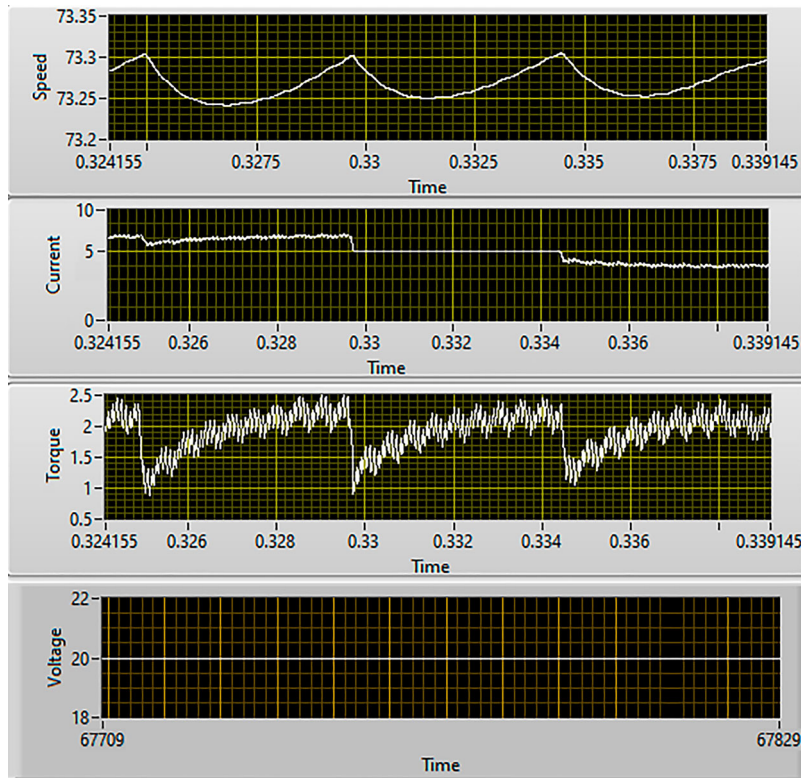


Figure 15: PV current (A), PV voltage (V), DC motor Torque (Nm) and speed (rad/s) with varying irradiance levels ($500\text{W}/\text{m}^2$ to $750\text{W}/\text{m}^2$)

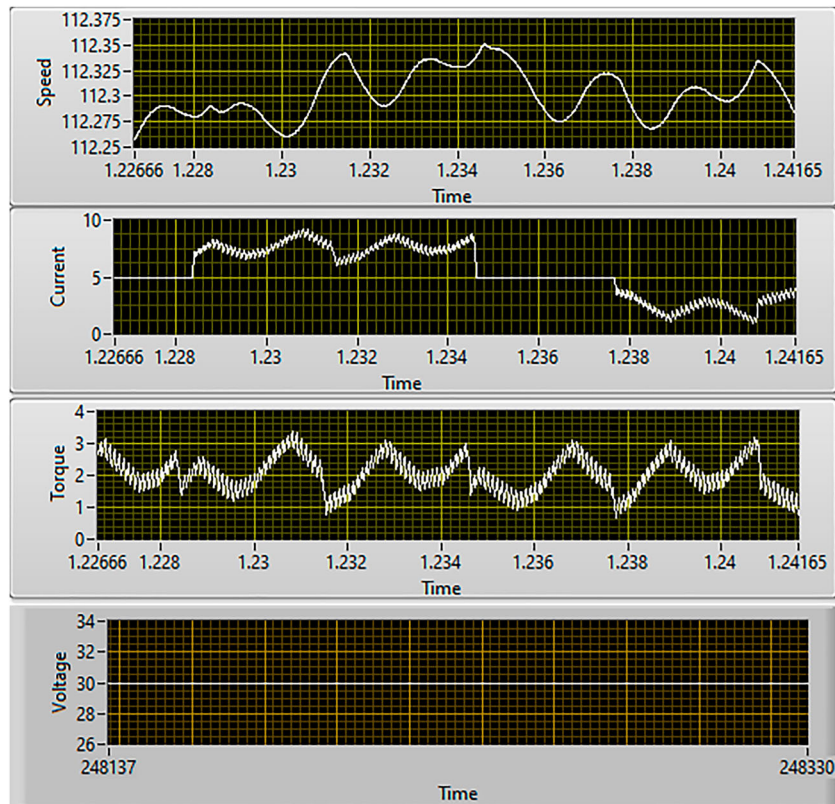


Figure 16: PV current, PV voltage, DC motor Torque and speed with varying irradiance levels ($400\text{W}/\text{m}^2$ to $1100\text{W}/\text{m}^2$)

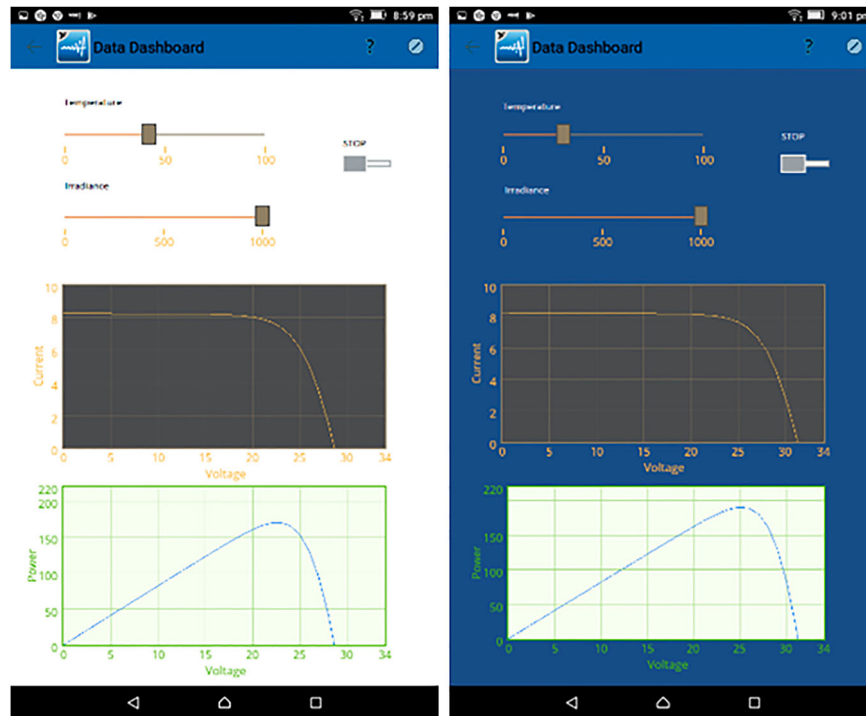


Figure 17: LabVIEW-based Data Dashboard

system's modeling, design, and simulation were carried out in a LabVIEW-based GUI environment. In supervised learning, the ANN controller learns from experience and is more responsive than the PID, Fuzzy, and FPID controllers. From Table 2, it has been depicted that by the use of ANN, no overshoot is present in the output, 64.82% improvement in settling time, 2.5% improvement in Damping Ratio, 7.6% improvement in Peak time, 15.78% improvement in Rise time as compared to FPID controller in speed control of DC motor applications. ANN controller has a significant improvement in the transient and steady-state response of the system over FPID, Fuzzy, and PID controller. Data dashboard and NI WSN are a good choice for wireless monitoring of the system.

ACKNOWLEDGMENTS

The authors acknowledge the NI Academy, Electronics & Communication Department, KIET Group of Institutions, Ghaziabad, Power Electronics Lab, Electrical Engineering Department, National Institute of Technology, Kurukshetra, India, for their assistance.

DISCLOSURE STATEMENT

No potential conflict of interest was reported by the author(s).

REFERENCES

1. R. Faranda, and S. Leva, "Energy comparison of MPPT techniques for PV systems," *WSEAS Trans. Power Syst.*, Vol. 3, pp. 446–455, 2008.
2. A. Dolara, R. Faranda, and S. Leva, "Energy comparison of seven MPPT techniques for PV systems," *J. Electromagnet. Anal. Appl.*, Vol. 3, pp. 152–162, 2009. doi:10.4236/jemaa.2009.13024
3. M. Chandrasekar, and T. Senthil kumar, "Experimental demonstration of enhanced solar energy utilization in flat PV (photovoltaic) modules cooled by heat spreaders in conjunction with cotton wick structures," *Int. J. Eng. Technol. Energy*, Vol. 90, pp. 1401–1410, 2015.
4. T. T. Chow, "A review on photovoltaic thermal hybrid solar technology," *Appl. Energy*, Vol. 87, no. 2, pp. 365–379, 2010. doi:10.1016/j.apenergy.2009.06.037
5. B. J. Huang, *et al.*, "Performance evaluation of solar photovoltaic thermal systems," *Sol. Energy*, Vol. 70, no. 5, pp. 443–448, 2001. doi:10.1016/S0038-092X(00)00153-5
6. National Instruments LabVIEW 2013 Help. Part Number 371361K-01, Edition June 2013.
7. K. Jaiganesh, and K. Duraiswamy, "Improving the power generation from solar PV panel combined with solar thermal system for Indian climatic condition," *Int. J. Appl. Environ. Sci.*, Vol. 6, pp. 763–776, 2013.

8. J. P. Singh, "Comparison of glass/glass and glass/ back-sheet PV modules using bifacial silicon solar cells," *IEEE J. Photovoltaic*, Vol. 5, no. 3, pp. 783–791, 2015. doi:10.1109/JPHOTOV.2015.2405756
9. N. S. Chauhan, A. K. Gupta, and R. Saxena, "Development of virtual laboratory for simulation and performance analysis of PV system," *Int. J. Res. Emerg. Sci. Technol.*, Vol. 2, pp. 177–182, 2015.
10. S. Tarak, *et al.*, "Matlab/Simulink based modeling of photovoltaic cell," *Int. J. Renewable Energy Res.*, Vol. 2, no. 2, pp. 213–218, 2012.
11. S. Samkeliso, and M. Hanif, "Comparative analysis of different single-diode PV modeling methods," *IEEE J. Photovoltaic*, Vol. 5, no. 3, pp. 938–946, 2015. doi:10.1109/JPHOTOV.2015.2395137
12. W. Y. Ying, "Performance analysis of photovoltaic –thermoelectric hybrid system with and without glass covers," *Energy Convers. Manage.*, Vol. 93, pp. 151–159, 2015. doi:10.1016/j.enconman.2015.01.013
13. K. P. Ramachandran. *Control engineering*. Noida: Wiley Precise Textbook, 2011.
14. R. Antonello, M. Carraro, A. Costabeber, F. Tinazzi, and M. Zigliotto, "Energy-Efficient Autonomous solar water-Pumping system for permanent-magnet synchronous motors," *IEEE Trans. Ind. Appl.*, Vol. 64, no. 1, pp. 43–50, 2017.
15. M. A. Husain, A. Tariq, S. Hameed, and MSBA, A Jain, "Comparative study of the reliability of MPPT algorithms for the crystalline silicon photovoltaic modules in variable weather conditions," *Green Energy Env.*, Vol. 2, pp. 5–17, 2017. doi:10.1016/j.gee.2016.11.001
16. W. M. M. Aung, Y. Win, and N. W. Zaw, "Implementation of solar photovoltaic Data monitoring system," *Int. J. Sci., Eng. Technol. Res.h (IJSETR)*, Vol. 7, pp. 591–596, Aug. 2018.
17. G. Remy, O. Bethoux, C. Marchand, and H. Dogan. "Review of MPPT Techniques for Photovoltaic Systems", 2018.
18. B. R. Copeland. "Using the LabVIEWPID Control Toolkit with the LabVIEW Control Design and Simulation Module", Sep. 2009.
19. M. Kamran, M. Mudassar, M. R. Fazal, M. U. Asghar, M. Bilal, and R. Asghar, "Implementation of improved Perturb & Observe MPPT technique with confined search space for standalone photovoltaic system," *J. King Saud Univ. – Eng. Sci.*, Vol. 1, no. 3, pp. 1–10, 2018.
20. S. Kouro, J. I. Leon, D. Vinnikov, and L. G. Franquelo, "Grid-connected photovoltaic systems: An overview of recent research and emerging PV converter technology," *IEEE Ind. Electron. Mag.*, Vol. 9, no. 1, pp. 47–61, Mar. 2015. doi:10.1109/MIE.2014.2376976
21. B. Tarroja, B. Shaffer, and S. Samuelsen, "The importance of grid integration for achievable greenhouse gas emissions reductions from alternative vehicle technologies," *Energy*, Vol. 87, pp. 504–519, Jul. 2015. doi:10.1016/j.energy.2015.05.012
22. M. K. Mishu, *et al.*, "An adaptive TE-PV hybrid energy harvesting system for self-powered IoT sensor applications," *Sensors*, Vol. 21, no. 8, pp. 2604, Apr. 2021. doi:10.3390/s21082604
23. T. Eswam, and P. L. Chapman, "Comparison of photovoltaic array maximum power point tracking techniques," *IEEE Trans. Energy Convers*, Vol. 22, no. 2, pp. 439–449, Jun. 2007. doi:10.1109/TEC.2006.874230
24. C. H. Basha, and C. Rani, "Different conventional and soft computing MPPT techniques for solar PV systems with high step-up boost converters: A comprehensive analysis," *Energies*, Vol. 13, no. 2, pp. 371, Jan. 2020. doi:10.3390/en13020371
25. J. M. Lopez-Guede, J. Ramos-Hernanz, N. Altin, S. Ozdemir, E. Kurt, and G. Azkune, "Neural modeling of fuzzy controllers for maximum power point tracking in photovoltaic energy systems," *J. Electron. Mater.*, Vol. 47, no. 8, pp. 4519–4532, Aug. 2018. doi:10.1007/s11664-018-6407-2
26. R. Divyasharon, R. N. Banu, and D. Devaraj. "Artificial neural network based MPPT with CUK converter topology for PV systems under varying climatic conditions" in Proc. IEEE Int. Conf. Intell. Techn. Control, Optim. Signal Process (INCOS), Apr. 2019, pp. 1–6.
27. L. Robert, and D. Boylestad. *Louis electronic devices and circuit theory*. 9th ed. New Jersey: Prentice Hall. 2008.
28. N. Savita, R. K. Nema, and G. Agnihotri, "Matlab/simulink based study of photovoltaic cells/modules/array and their experimental verification," *Int. J. Energy Environ.*, Vol. 1, no. 3, pp. 487–500, 2010.
29. I. Mahmud, *et al.*, "Novel technique in characterizing a PV module using pulse width modulator," *Int. J. Res. Eng. Technol. (IJRET)*, Vol. 2, pp. 173–177, 2015.
30. N. M. A. A. Shannan, N. Z. Yahaya, and B. Singh. "Single-diode model and two-diode model of PV modules: a comparison" in IEEE International Conference on Control System, Computing and Engineering, 2013, Penang, Malaysia, 2013, pp. 210–214.
31. V. Tamrakar, S. C. Gupta, and Y. Sawle, "Single-diode and two-diode PV cell modelling using Matlab for studying characteristics of solar cell under varying," *Electr. Comput. Eng.: An Int. J. (ECIJ)*, Vol. 4, no. 2, pp. 5–17, 2015.

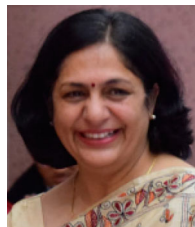
32. P. Das, "Maximum Power Tracking Based Open Circuit Voltage Method for PV System," *Energy Procedia*, Vol. 90, pp. 2–13, 2016. doi:10.1016/j.egypro.2016.11.165.
33. B. Singh, A. K. Mishra, and R. Kumar, "Solar powered water pumping system employing switched reluctance motor drive," *IEEE Trans. Ind. Appl.*, Vol. 52, no. 5, pp. 3949–3957, 2016. doi:10.1109/TIA.2016.2564945
34. T. L. Nguyen, and K. Low, "A global maximum power point tracking scheme employing DIRECT search algorithm for photovoltaic systems," *IEEE Trans. Ind. Electron.*, Vol. 57, no. 10, pp. 3456–3467, Oct. 2010. doi:10.1109/TIE.2009.2039450
35. J. Ahmed, and Z. Salam, "An improved perturb and observe (P & O) maximum power point tracking (MPPT) algorithm for higher efficiency," *Appl. Energy Elsevier*, Vol. 150, pp. 1–10, 2015. doi:10.1016/j.apenergy.2015.04.013
36. A. K. Gupta, Y. K. Chauhan, and T. Maity, "Experimental investigations and comparison of various MPPT techniques for photovoltaic system," *Indian Acad. Sci.*, Vol. 43, no. 132, pp. 1–15, 2018.
37. J Salim, "Ohri "controlling of solar powered S.E DC motor using IMC controller," *WSEAS Trans. Power Syst*, Vol. 14, pp. 65–69, 2019.
38. J. V. M. Caracas, G. d. C. Farias, L. F. M. Teixeira, and L. A. d. S. Ribeiro, "Implementation of a high-efficiency, high-lifetime, and low-cost converter for an autonomous photovoltaic water pumping system," *IEEE Trans. Ind. Appl.*, Vol. 50, no. 1, pp. 631–641, 2014. doi:10.1109/TIA.2013.2271214
39. A. Sahbel, N. Hassan, M. M. Abdelhameed, and A. Zekry, "Experimental performance characterization of photovoltaic modules using DAQ," *Energy Procedia*, Vol. 36, pp. 323–332, 2013. <http://dx.doi.org/10.1016/j.egypro.2013.07.037>.
40. A. Yousry, M. Zahran, and A. Al-Hossain, "Solar cell curves measurement based on LabVIEW microcontroller interfacing," *Proceedings of the 12th WSEAS International Conference on Automatic Control Modeling and Simulation*, 2010.
41. A. Aristizabal, "Development of equipment for monitoring PV power plants, using Virtual Instrumentation," *Photovoltaic Energy Conversion, Conference Record of the 2006 IEEE 4th World Conference*, Vol. 2, 2006.
42. R. Kumar, and B. Singh, "BLDC motor-driven solar PV array-fed water pumping system employing zeta converter," *IEEE Transactions on Industry Applications*, Vol. 52, no. 3, pp. 2315–2322, 2016. doi:10.1109/TIA.2016.2522943.
43. S. Shukla, and B. Singh, "Single-stage PV array fed speed sensorless vector control of induction motor drive for water pumping," *IEEE Transactions on Industry Applications*, Vol. 54, no. 4, pp. 3575–3585, 2018. doi:10.1109/TIA.2018.2810263.

AUTHOR



Salim received his B.Tech from the Department of Instrumentation (USIC), Kurukshetra University, and M.Tech from the National Institute of Technology Kurukshetra. Presently he is doing a Ph.D. from the National Institute of Technology Kurukshetra. He currently is an Assistant Professor in the Electrical & Electronics Engineering Department, KIET Group of Institutions Delhi-NCR Ghaziabad, India. His area of interest includes control system, Renewable Energy, Microprocessor and Microcontroller-based applications. Mr. Salim is a Certified LabVIEW Associate Developer (CLAD).

Corresponding author. Email: salimnitk@gmail.com, salim@kiet.edu



Dr. Jyoti Ohri received her B.Tech, M.Tech, and Ph.D. from the National Institute Technology Kurukshetra, India. She is presently Professor in the Electrical Engineering Department, National Institute of Technology Kurukshetra, India. Her area of interest includes robotics, optimal robust and intelligent control, etc. She has vast teaching and research experience in her account. She holds various research, academics and administrative position at a different level. She has numerous research articles in various Journals and Conferences. She is a reviewer of various Journals. Prof. Ohri is a member of various reputed professional societies, such as IEEE, IEEE Control System Society, and IEEE Computer Society Technical Community on Haptics.

E-mail: ohrijyoti@rediffmail.com